

Multimessenger Observations of Neutron Star Merger GW170817

Justin Flaherty

The Ohio State University, Department of Physics

(Dated: August 4, 2020)

Abstract

Virgo and LIGO detected and localized a gravitational wave candidate (GW170817) on 2017 August 17 12:41:04 UTC, while Fermi-GBM detected and localized a gamma-ray burst candidate (GRB 170817A) in the same localization region two seconds later. This signal was consistent with the coalescence of a binary neutron star merger with a merger time of 12:41:04 UTC and sparked a global observation of the region for electromagnetic and neutrino signals. EM observations detected an optical transient consistent with models of kilonovae. No neutrino candidates were discovered, primarily due to a large off-axis viewing angle from the jet axis. This is the first time a source has emitted GW and EM signals, and the implications of which has lead to advancements in multi-messenger astronomy.

CONTENTS

I. Introduction	3
II. Initial Observations	3
A. Gravitational Waves	5
B. Gamma-Ray Burst	8
C. Optical Transient	9
III. Electromagnetic Follow-Up	11
A. Optical, Ultraviolet, Infrared	12
B. Gamma-Rays	13
C. X-Ray	13
D. Radio	14
IV. Neutrino Search	14
A. IceCube	15
B. ANTARES	16
C. Pierre Auger Observatory	17
V. Implications for Physics	18
VI. Conclusions	20
References	21

I. INTRODUCTION

On 2017 August 17, a Gravitational Wave (GW) candidate for the coalescence of a binary system was detected at 12:41:04 UTC. Two seconds later a short-lived Gamma-Ray Burst (GRB) was detected and localized in the same region as the binary merger. This implied the merger event was that of a Binary Neutron Star (BNS) system, a yet unobserved event. This serves as the first ever gravitational wave with an Electromagnetic (EM) counterpart, sparking observations across the entire EM spectrum as well a search for neutrinos. This event is highly significant, as the EM counterpart allows for further understanding of GW sources and the propagation of GWs. This merger also left behind an optical transient, whose emission fits theoretical models of a kilonova [8].

A timeline of GW and EM observations is available in Figure 1, while no coincident neutrino candidates were detected. Following the natural progression of observation outlined by [8], the observation and results are presented in this paper. In Section II we discuss the initial observations of gravitational waves, gamma-rays, and the detection of an optical transient. Section III covers the subsequent follow-up search across the electromagnetic spectrum and the search for neutrinos. The implications of this event and how it impacts physics is discussed in Section V.

II. INITIAL OBSERVATIONS

On the first day of observation, the gamma-ray and gravitational wave signals were detected independently. Both observations were sent out as Gamma-ray Coordinates Network (GCN) notices prompted further electromagnetic observation that identified and localized an optical transient. In this section, the instrumentation used and the method of detection will be discussed; as well as the results. A full timeline of these observations is available in Figure 1.

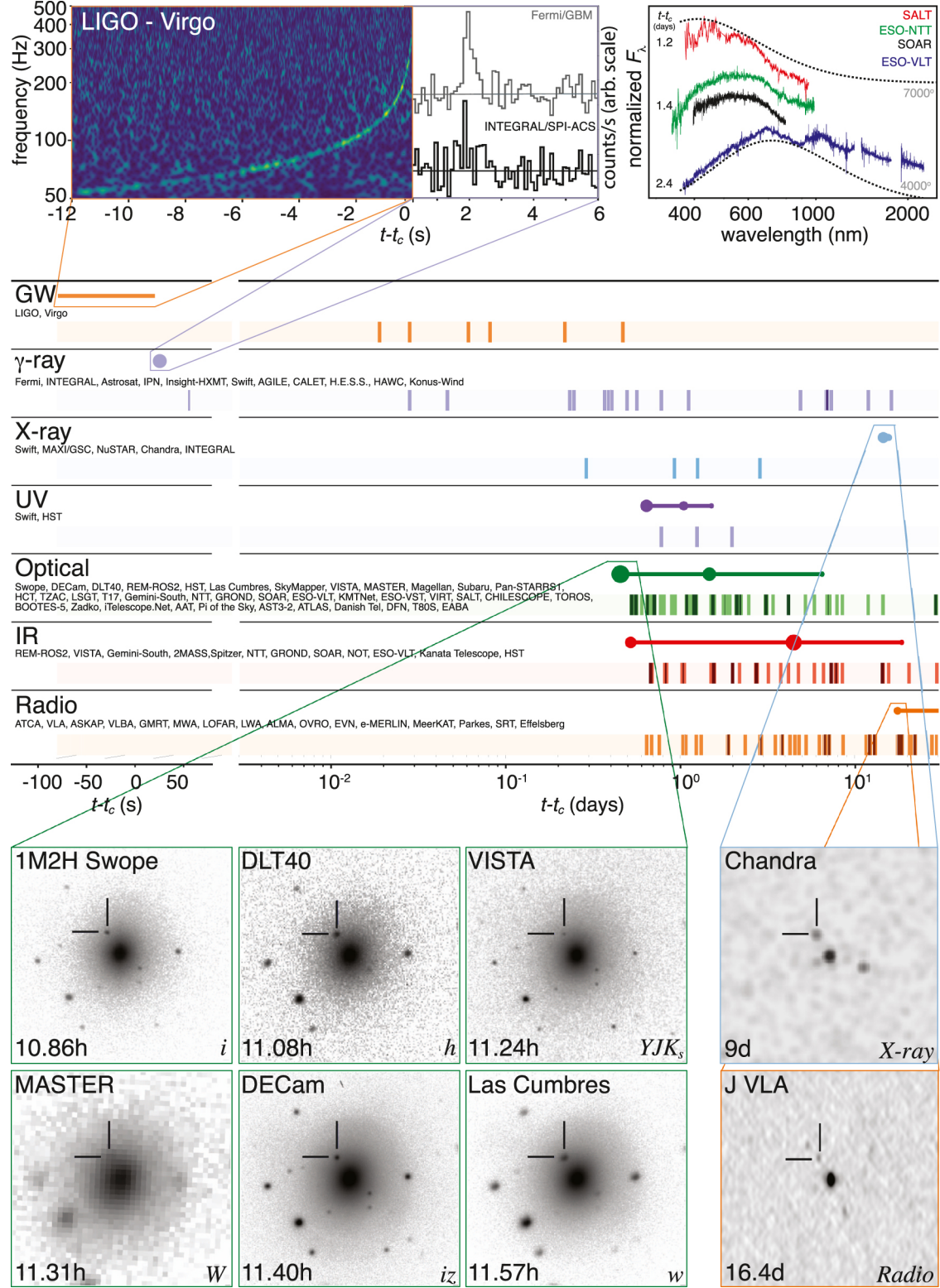


FIG. 1: Timeline of the discovery of GW170817, GRB 170817A, and SSS17a/AT 2017gfo; as well as the subsequent follow-up observations relative to the merger time t_c . The the rows are separated by the observation band (gravitational and electromagnetic), and the names of the relevant instruments and observing teams are given in each row. The shaded dashes represent times when the information was reported in a GCN circular. Representative observations in each band are shown with solid circles, with the size approximately scaled with their brightness. Solid lines indicate when the source was detectable by at least one telescope. Samplings of the measured signal are given by the subplots with lines highlighting their placement on the timeline. [8]

A. Gravitational Waves

Three detectors were involved with the observation of GW170817: LIGO-Hanford, LIGO-Livingston, and Virgo. The detectors at LIGO-Hanford and LIGO-Livingston have similar designs, the basis of which is a Michelson Interferometer with a Fabry-Perot resonant cavity in each arm that increases the optical path by a factor of 500 [4]. This cavity serves to increase the phase shift produced by a shift in the arm length, as the strain from gravitational waves are on order of 10^{-20} [22] and thus produce small phase shifts without the cavity. Both detectors have arm lengths of 3994.5 m and utilize a linearly polarized Nd:YAG laser operating at 1064 nm and a power of up to 125 W [4]. Virgo has a similar design to that of LIGO, where it is a large Michelson Interferometer with 3 km arms each containing a Fabry-Perot cavity that increase the optical path by a factor of 30; and also uses a Nd:YAG laser operating at 1064 nm and a power of up to 10 W [9].

The signal first reached the Virgo detector at 12:41:04 UTC, followed by LIGO-Livingston 22 ms later, and then LIGO-Hanford after another 3 ms; as shown in Figure 2. It was initially detected as a single-detector event by LIGO-Hanford, but manual analysis of the LIGO-Livingston data showed a detection that was masked by short instrumental transient noise that plagues each detector independently every few hours as shown in Figure 3. The source of this noise is unknown and appears to have no temporal correlation between the two LIGO sites [7]. The low amplitude in the Virgo signal is due to a few factors: scattered light from the output optics above 150 Hz, seismic noise from anthropogenic activity below 30 Hz, noise excess around 50 Hz due to European power mains, having a lower BNS horizon relative to LIGO, and the direction of the source with respect to the antenna pattern. This low signal amplitude significantly constrained the sky position, but kept Virgo from making significant contributions to other parameters [7].

Combined analysis of the three signals yield a Signal-to-Noise Ratio (SNR) of 32.4; with values of 26.4, 18.8, and 2.0 for LIGO-Livingston, LIGO-Hanford, and Virgo, respectively. This makes it the hitherto loudest gravitational wave signal [7]. The Chirp Mass \mathcal{M} , a descriptor of the binary system that drives the frequency evolution of the signal at the

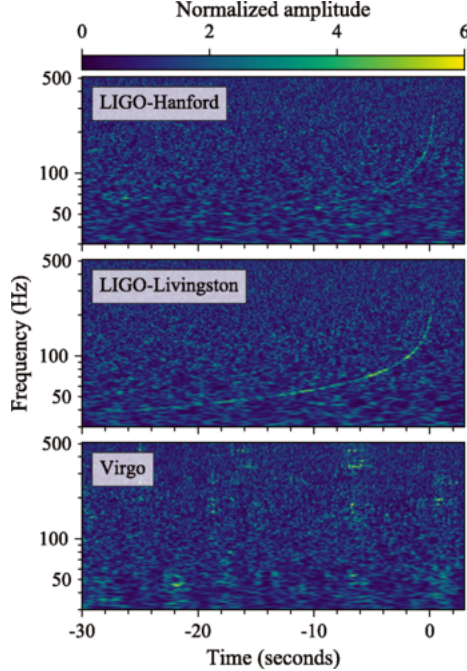


FIG. 2: Time-frequency plots of the data containing GW170817 from LIGO-Hanford, LIGO-Livingston, and Virgo. Times are show relative to the merger time of August 17, 2017 14:41:04 UTC. The non-detection of a signal in Virgo allowed for finer localization of the source. [7]

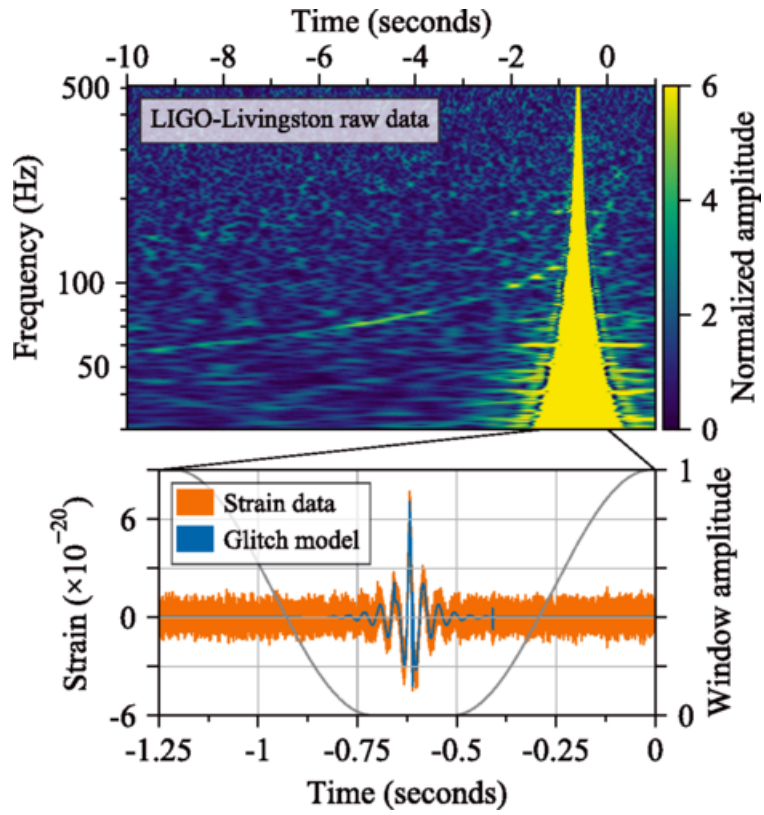


FIG. 3: Noise in the LIGO-Livingston data shown relative to the merger. The source of the noise is unknown. [7]

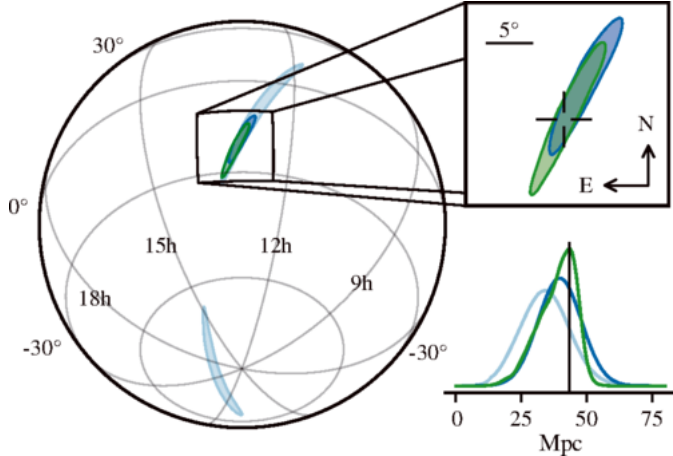


FIG. 4: Localization of GW170817 rapidly reconstructed from a Hanford-Livingston (190 deg^2 , light blue) and Hanford-Livingston-Virgo (31 deg^2 , dark blue) analysis. A higher latency Hanford-Livingston-Virgo analysis improved the localization (28 deg^2 , green). The recticle in the top-right panel marks the location of the host galaxy NGC 4993. The bottom-right panel showing the luminosity distance distribution from the three analyses, with the black line marking the accepted distance to NGC 4993. [7]

leading order, can be obtained from the time-frequency signal:

$$\mathcal{M} = \frac{c^3}{G} \left(\frac{5}{96} \pi^{-8/3} f^{-11/3} \dot{f} \right)^{3/5}. \quad (1)$$

Where $f = f(t)$ is the time-frequency signal, G is the universal gravitational constant, and c is the speed of light. This can then be used to obtain the individual masses of the system:

$$\mathcal{M} = \frac{(m_1 m_2)^{3/5}}{(m_1 + m_2)^{1/5}}. \quad (2)$$

From the signal, the chirp mass was found to be $\mathcal{M} = 1.188^{+0.004}_{-0.002} M_\odot$, where M_\odot is the solar mass. The component masses were found to be $m_1 = (1.36 - 2.26) M_\odot$ and $m_2 = (0.86 - 1.36) M_\odot$, which is further affected by the spin of the component stars [7].

The luminosity distance can be independently obtained from the gravitational wave signal, and it was found to be $D_L = 40^{+8}_{-14} \text{ Mpc}$. Combining the three signals allowed for a sky map to be generated, as shown in Figure 4. This limits the localization to a 28 deg^2 region in the sky, located within the galaxy NGC 4993. This host galaxy is further confirmed by the observation of an optical transient in Section II C.

B. Gamma-Ray Burst

Two detectors were involved with the initial detection of GRB 170817A: The INTErnational Gamma-Ray Astrophysics Laboratory (INTEGRAL) and the Fermi-GBM (Gamma-ray Burst Monitor) [8].

The INTEGRAL detector is a space-based observatory augmented with multiple instruments that cover different regions of the EM spectrum: SPI, a gamma-ray spectrometer; IBIS, an imager covering an energy range of 15 keV - 10 MeV; JEM-X, an X-ray monitor; and OMC, an Optical Monitoring Camera [27]. SPI (SPectrometer on Integral) was responsible for detection of the GRB and covers an energy range of 20 keV to 8 MeV. It is surrounded by a thick Anti-Coincidence Shield (SPI-ACS) that provides a veto signal for charged particles that irradiate the instrument and can register all impinging particles and high-energy photons. This allows it to serve as an omnidirectional detector with a time resolution of 50 ms and effective area of 0.7 m^2 at energies above 75 keV [27].

Fermi-GBM is another space-based detector that is on board the Fermi Gamma-Ray Space Telescope. It is composed of twelve thalium-doped sodium iodide scintillation detectors that cover an energy range of 8-1000 keV and are pointed at various angles across the sky, as well as two bismuth germanate crystals that cover an energy range of 200 keV - 40 MeV placed on opposite sides of the craft. Incoming photons interact with the detectors and create scintillating photons, which get collected by photomultiplier tubes and converted into an electronic signal [21].

The initial gamma-ray burst GRB 170817A was detected by INTEGRAL at 12:41:06.48 UTC for a period of 100 ms [27], followed by an autonomous detection by the flight triggering software of Fermi-GBM on a 256 ms accumulation from 50 to 300 keV ending at 12:41:06.474598 UTC [6, 21]. The time series of the signals shown relative to the gravitational wave signal can be seen in Figure 5. There is a noticeable time-delay of approximately 1.74 s between the gravitational wave signal and the gamma-ray burst, the implications of which are discussed in Section V. The signals were able to be used to create a skymap and localize the signal to a region that is coincident with the LIGO-Virgo localization region, as

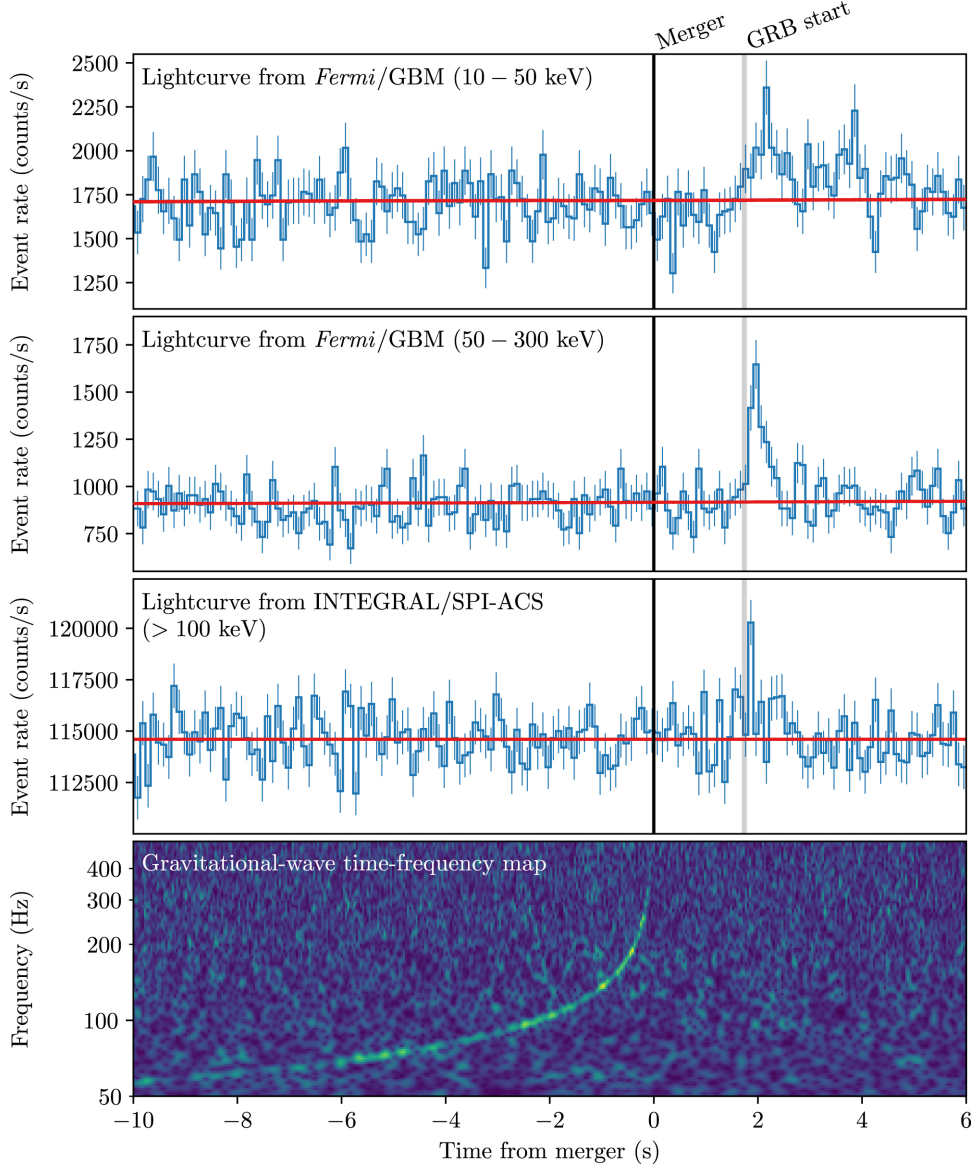


FIG. 5: Joint, multi-messenger detection of GW170817 and GRB 170817A. Top three plots represent the light curves for Fermi/GBM and INTEGRAL/SPI-ACS in energy ranges 10 - 50 keV, 50 - 300 keV, and > 100 keV. Bottom plot shows the time-frequency map of GW170817 obtained by coherently combining the signals from LIGO-Hanford and LIGO-Livingston. [6]

shown in Figure 6.

C. Optical Transient

After global notice was made from the detection of GW170817 and GRB 170817A, numerous optical telescopes were able to detect an optical transient left by the merger within the first day: The One-Meter, Two-Hemisphere (1M2H) team; Distance Less Than 40 Mpc (DLT40); the Visible and Infrared Survey Telescope for Astronomy (VISTA); the Mobile

Astronomical System of TElescope Robots (MASTER) Project; Dark Energy Camera (DE-Cam); and Las Cumbres Observatory (LCO) [8]. The images for each of these observations are shown as the green-bordered plots on the bottom of Figure 1.

1M2H was the first to discover the optical transient 10.87 hr post-merger using the 1 m Swope telescope at the Las Campanas Observatory in Chile [8, 17]. This was accomplished by using a catalog of nearby galaxies that fall within common localization region obtained by the GW and GRB measurements to create a prioritized list of the 100 most-probable host galaxies. Forty-six galaxies were able to be combined into a series of 12 images, while the remaining candidates had to be isolated to their own images. NGC 4993 had shown a high magnitude optical source in near-infrared that was not in any archival imaging as shown in Figure 6, where the upper-right plot shows the host galaxy post-merger, while the lower-right shows it pre-merger [17]. The transient is highlighted by the crosshairs in the upper-right plot. This transient was dubbed SSS17a (later AT 2017gfo), and was located at Right Ascension α ($J2000.0$) = $13^h09^m48^s.085 \pm 0.018$ and Declination δ ($J2000.0$) = $-23^\circ22'53''.343 \pm 0.218$ [17].

DLT40 was the second to observe the transient, and managed to do so independently of 1M2H [8]. This observatory is a one-day cadence supernova search that uses a 0.4 m optical telescope located at the Cerro Tololo Inter-American Observatory, observing up to 600 targeted galaxies on a nightly basis. Following the global alert for GW170817 and GRB 170817A, DLT40 was directed to the initial LIGO-Virgo localization region and prioritized 20 galaxies within the 99% confidence region as well as the 31 most luminous galaxies in the Fermi region. At 11.08 hr post-merger, the transient was located in near-infrared at α ($J2000.0$) = $13^h09^m48^s.09$ and δ ($J2000.0$) = $-23^\circ22'53''.46$, slightly offset from the center of NGC 4993, and was designated DLT17ck (later AT 2017gfo) [30].

VISTA is a 4 m specialized wide field telescope in the European Southern Observatory. Two fields within the GW error region and containing high densities of galaxies within the initial luminosity distance. Similar to the method used by 1M2H, a bright new point source in near-infrared was detected at α ($J2000.0$) = $13^h09^m48^s.09$ and δ ($J2000.0$) = $-23^\circ22'53''.3$ that did not appear in prior imaging of the region.

MASTER is a robotic system of visible telescopes near Moscow whose purpose is to provide prompt observations of gamma-ray bursts. It is fully autonomous, using GCNs to provide coordinates for observation and carrying out an early afterglow search of the region [24]. At the time of the GCN it was nighttime in Moscow, so a follow-up search could not be conducted until the following day. The transient was able to be detected in the visible range 11.31 hr post-merger [25].

DECam is a near-infrared imager installed on the 4 m Victor M. Blanco telescope at the Cerro Tololo Inter American Observatory with the primary goal of studying the nature of dark energy [20]. The LIGO-Virgo localization region was visible within 90 minutes of the merger, so overnight observation with 30 s exposures began. A visual inspection of raw images compared to archival data lead to the discovery of a new source near NGC 4993 that was imaged 11.40 hr post-merger [28].

The Las Cumbres Observatory is a network of telescopes located in six sites operational at the time of the merger: the Cerro Tololo Interamerican Observatory in Chile, the South African Astronomical Observatory, the Siding Spring Observatory in Australia, the McDonald Observatory in Texas, the Haleakala Observatory in Hawaii, and the Teide Observatory in the Canary Islands; using a collection of 2 m, 1 m, 83 cm, and 40 cm telescopes [16]. Five hours after the localization region was issued, Las Cumbres performed a galaxy-targeted follow-up that prioritizes galaxies that were at higher-probability locations within the region that have a higher intrinsic luminosity in the blue-visible band (which indicates a higher mass). The transient was discovered 11.57 hr post-merger, and was consistent with the host galaxy of NGC 4993 [14].

III. ELECTROMAGNETIC FOLLOW-UP

A massive follow-up observation campaign was conducted on the transient over the weeks following the merger, observing across the entire electromagnetic spectrum. This eventually lead to the discovery of X-ray and radio counterparts to the signal [8]. Numerous observatories participated in this campaign and are listed based on the spectral band in Figure 1.

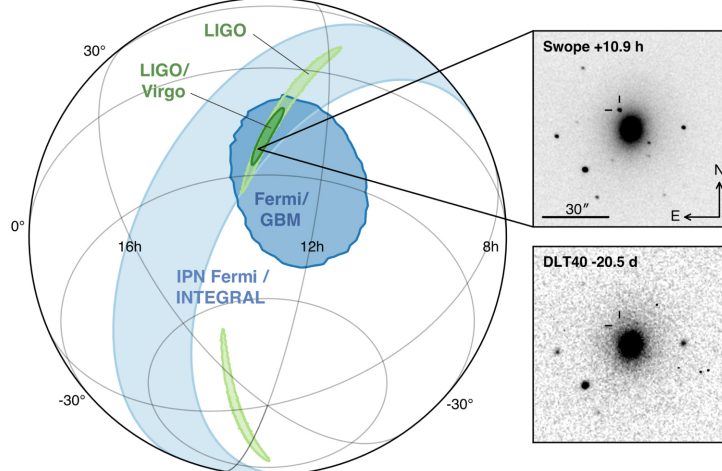


FIG. 6: Localization of the gravitational-wave, gamma-ray, and optical signals from LIGO, Virgo, Fermi, and INTEGRAL. Light green represents the 90% credible regions for LIGO (190 deg^2); dark green is the initial LIGO-Virgo localization (31 deg^2); the IPN triangulation from the time delay between Fermi and INTEGRAL is light blue, while Fermi-GBM is dark blue. The overlapping regions identify the host galaxy of NGC 4993 with the Swope optical image 10.9 hr after coalescence and DLT40 optical image 20.5 days prior to coalescence, showing that the transient did not exist prior to the merger. [8]

For the sake of brevity, only the most prominent observations will be discussed.

A. Optical, Ultraviolet, Infrared

Observations spanning the visible, ultraviolet, and infrared regions of the electromagnetic spectrum were conducted with 46 instruments and 37 unique filters spanning from 0.45 days to 29.4 days post-merger. Between 11.6 hr and 15.3 hr post-merger, observations constrained the early optical observations to be in the near-infrared with a bright ultraviolet component which helped constrain the effective temperature of the remnant [31]. The next few days showed a rapid fall off in the blue spectrum without any individual features identifiable to a supernova. This helped rule out the possibility of a chance coincidence of GRB 170817A being separate from GW170817 [8].

Additionally this event showed a rapid cooling without commonly observed ions from elements that are abundant in supernova ejecta, making this object heretofore unseen in its optical emission, making it broadly indicative of a kilonova. Models of kilonovae predict rapid shifts in energy distribution from the optical to near-infrared, which is illustrated in Figure 7. These spectroscopic observations have lead to the conclusion that this source broadly matches theoretical predictions of kilonovae [8, 31].

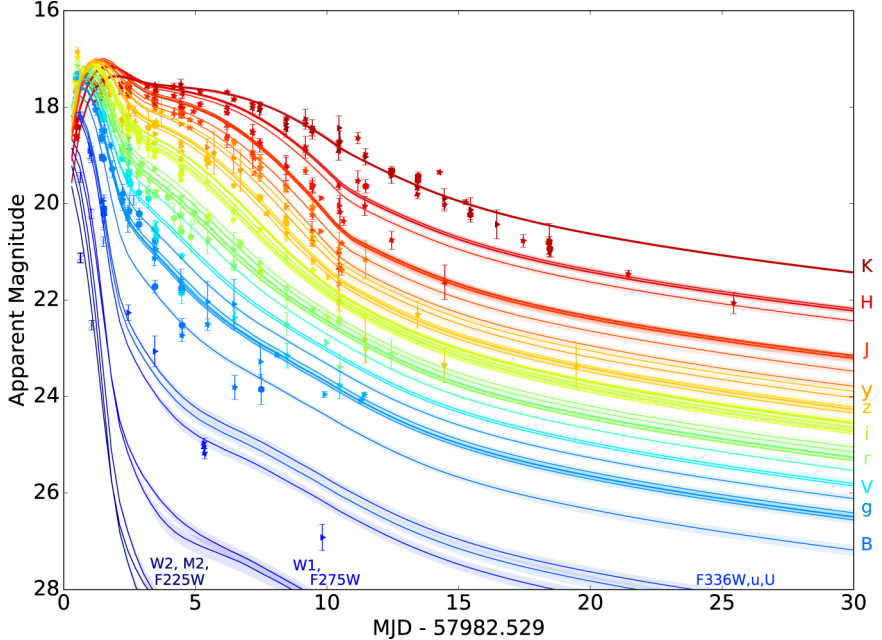


FIG. 7: Light curves covering UVOIR compiled by [31]. The horizontal axis shows time since the merger in units of Modified Julian Date (MJD), where 57982.529 is the merger time and each integer tick represents one day. Optical bands use the photometric system.

B. Gamma-Rays

Follow-up observations of gamma-rays utilized the Earth Occultation technique, which involves a large area of detectors sensitive to photons above 20 keV. Some detectors had an unfavorable orientation, but Fermi-GBM was able to maintain uninterrupted observation of the site for 10 hours post-merger. This allowed SPI-ACS to rule out a steady source that was ten times weaker than the prompt emission of GRB 170817A. Other detectors were able to monitor the site surrounding the merger (AGILE, LAT, H.E.S.S., HAWC, and INTEGRAL), however none of them found evidence of sustained gamma-ray afterglow following the merger, likely due to the large off-axis angle [8, 27].

C. X-Ray

X-ray observations were conducted as they help constrain the geometry of the outflow, its energy output, and the orientation of the remnant with respect to line of sight [8]. The transient was initially not visible in X-ray, but Chandra was able to begin observation seven days post-merger and detected a faint X-ray source at the location of the merger, as seen in

the blue-bordered image in Figure 1. Observations by Chandra five days later confirmed the presence of continued X-ray activity. Basic models for kilonovae do not predict detectable X-ray emission, but previous candidate kilonovae exhibited X-ray brightening [29].

In order to confirm that the short GRB and the GW source are co-located, possible X-ray emitters must be ruled out. Fast moving ejecta within the remnant material could produce emission, but an ambient density of $n > 10^3 \text{ cm}^{-3}$ is necessary. Optical measurements show no evidence of this density at the time of detection. A rapidly rotating and highly magnetized neutron star could generate emission, but no current models can produce persistent emission over a time scale of two weeks. Thermal spectral measurements also rule out the possibility of fallback accretion. Thus the only source of X-ray emission is synchrotron afterglow radiation from the short GRB 170817A. This conclusion is further justified by the detection of radio emission within the same synchrotron regime [29].

D. Radio

Radio emissions from this event assist in the tracing of fast-moving ejecta from the merger, allowing us to investigate the energetics of the explosion, the geometry of the ejecta, and the environment of the merger [8]. The first radio detection consistent with the source location occurred 16 days post-merger by the Very Large Array (VLA), which can be seen as the orange-bordered image in Figure 1 [8, 13]. Observations were continued by the VLA as well as the Australia Telescope Compact Array (ATCA) covering a period of 125 - 200 days post-merger and found that the radio afterglow peaked at 149 ± 2 days post-merger with a steady decline in flux after. This is consistent with the evolution of a synchrotron emitting in the radio, optical, and X-ray regimes [18].

IV. NEUTRINO SEARCH

The merger prompted a search for neutrino candidates coincident with the source by IceCube, ANTARES, and Pierre Auger Observatory. All candidates that were measured within

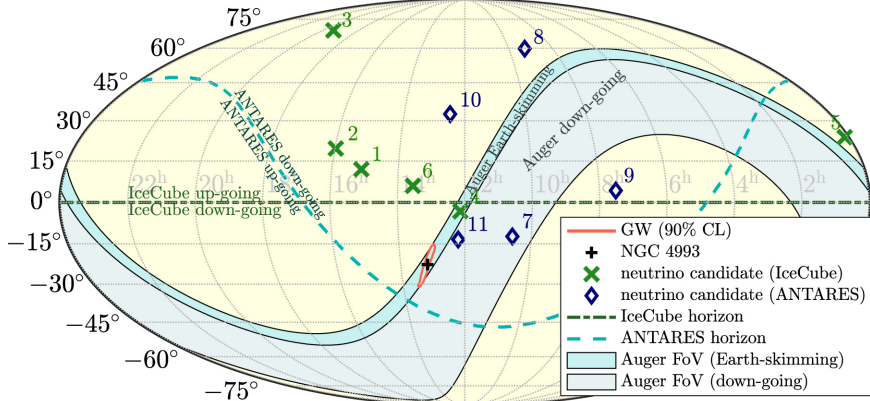


FIG. 8: Skymap of the localization of sensitive areas at the time of GW170817. The red curve represents the 90% credible region as found in [7], with the black plus representing the location of the host galaxy as found in [17]. The green crosses and blue diamonds represent the neutrino candidates for IceCube and ANTARES, respectively, in a 500 s window surrounding the merger. No candidates were found to be correlated with the BNS merger. [12]

a ± 500 s window surrounding the merger are shown in Figure 8 with their sky positions shown relative to the event. No neutrino candidates were found to be coincident, primarily due to the large off-axis viewing angle relative to the jet axis [12], which is visualized in Figure 9. As the observation angle relative to the jet-axis gets larger, the neutrino fluence drastically grows weaker as shown in Figure 10. The large off-axis angle of approximately 36° means that the non-detection of neutrino candidates was expected [12].

A. IceCube

The IceCube detector is a cubic kilometer of ice located 1450 m below the South Pole that has been turned into a Cherenkov detector. It is outfitted with 5160 digital optical modules (DOMs), each containing a 10-inch photomultiplier and electronics board to locally digitize the signal within two nanosecond accuracy [11]. Following the detection of GW170817, IceCube performed a search for neutrino signals using two different event selection techniques.

The first technique involved an online selection of through-going muons that primarily identifies cosmic-ray-induced background events [2, 3]. For every 1000 seconds, this technique has an expectation of 4.0 events in the northern sky, and 2.7 in the southern sky [12]; with the merger occurring in the southern sky. This method found six events within a ± 500 s time window as shown in Figure 8, but none were found to be spatially or temporally correlated with the merger.

The second technique filters out atmospheric background events with the help of the outermost optical sensors in the instrumented volume. By using the outermost sensors as a veto layer, events that trigger the outermost layer will be filtered out. This limits detection to events that occur within the volume of IceCube. This method of selection has a more variable event rate across the sky, but is overall much lower compared to the first one [12]. During the $\pm 500s$ window surrounding the merger, no events passed this method of selection [12].

With a 99.88% duty cycle, IceCube was able to maintain continuous exposure on the source location for the 14 day observation period and measure six events, but none were coincident with the merger. This is due to two factors, first being that the merger was observed at a large off-axis angle, so detectors were not within the line of sight. The second factor is due to a low neutrino energies, as shown in Figure 8 [12].

B. ANTARES

The Astronomy with a Neutrino Telescope and Abyss environmental RESearch project (ANTARES) is a neutrino telescope that operates in the Mediterranean sea. It is a three-dimensional array of optical modules housing photomultiplier tubes that search for Cherenkov radiation from neutrino-muon interactions. It is sensitive to up-going and down-going neutrinos with energies of at least 100 GeV [10].

The location of the merger was outside of the up-going sensitive region of ANTARES, so the search was limited to down-going neutrinos. This search was done by suppressing the background affecting the dataset by requiring a space and time coincidence with the event. From this method five background events were found, but were not compatible with the source position and were likely atmospheric events [12].

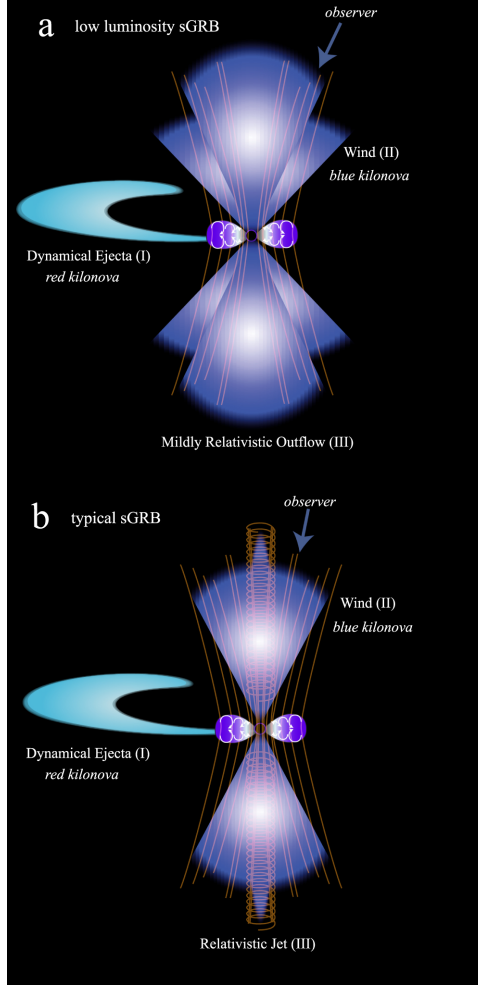


FIG. 9: Overview of main energy transfer processes believed to be involved in ejecting material in the creation of a short Gamma-ray Burst (sGRB) via BNS merger. A small percentage of the matter is ejected in the form of a tidal tail (I). The merged remnant is expected to produce strong winds (II). The expected result is the collapse into a black hole, which would produce a relativistic jet (III in b). A large amount of entrained baryonic mass can severely limit the relativistic outflows, leading to lower luminosity sGRB (III in a). This figure shows the observer to be offset from the jet axis, which is the case of GRB 170817A. [26]

C. Pierre Auger Observatory

The Pierre Auger Observatory is a surface detector in Argentina consisting of 1660 water-Cherenkov stations positioned over an approximately 3000 km^2 area, with 1.5 km grid spacing. It detects atmospheric particle showers induced by ultra-high energy neutrinos with energies above 10^{17} eV in intervals of 25 ns. These particle showers are dominated by muons that form sharp time traces in the water-Cherenkov stations [1, 12]. Auger performed a search for neutrino candidates in a $\pm 500 \text{ s}$ surrounding the merger, as well as 14 days following it. NGC 4993 was visible in Auger's field of view and it search for two types of neutrinos: Earth-skimming and down-going.

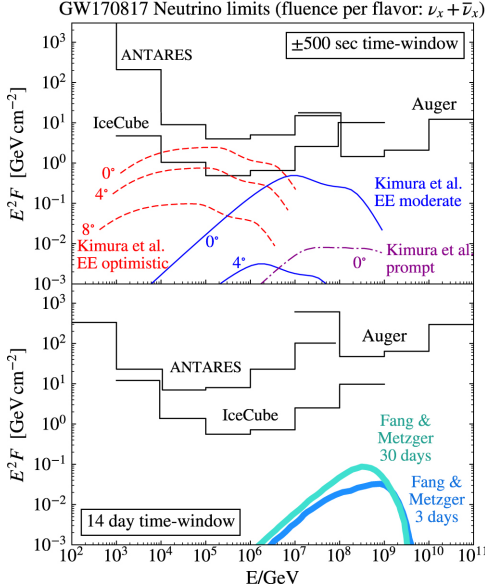


FIG. 10: Top: Upper limits on the neutrino spectral fluence from GW170817 for each experiment (black) in a 500 s window around the merger. Predictions for neutrino emission for prompt emission and extended emission (EE) from [23] are given as well, characterized by the observation angle with respect to the jet axis to show its dependence. GW data and the redshift of NGC 4993 constrain the observation angle to be within 36° . Bottom: Upper limits on the neutrino spectral fluence from GW170817 for each experiment (black) over a 14 day period after the merger. Models from [19] are scaled to a distance of 40 Mpc. [12]

The first method searched for Earth-skimming showers induced mainly by tau neutrinos that traverse below the Earth's crust and induces a tau lepton that escapes the Earth and decays above the surface detector. During the 500 s window and 14-day period, no events passed this method of detection. This absence of Earth-skimming neutrinos allowed constraints to be placed on the fluence of ultra-high energy neutrinos from GW170817 [12].

The second method searches for down-going neutrinos that undergo a muon interaction after penetrating much of the atmosphere. Cosmic-ray muons are less likely to reach the surface detector as they are likely to get absorbed within the atmosphere. A neutrino-muon interaction will create a particle shower near ground-level and induce sharp time traces in the water-Cherenkov stations. No neutrino candidates with this method [12].

V. IMPLICATIONS FOR PHYSICS

This BNS merger was the first to be observed with both gravitational and electromagnetic waves. This allowed for analysis of the speed of gravity versus the speed of light, the testing of the equivalence principle for the propagation of electromagnetic waves and gravitational

waves, measuring the Hubble constant independent of the Cosmic Microwave Background, and evaluating the local coalescence rate of BNS systems.

It has been long thought that gravitational waves propagate at the speed of light, but an arrival delay of $(1.74 \pm 0.05) \text{ s}$ between the GW signal and light signal (when accounting for the time delay between emissions) [6] suggest otherwise. The fractional difference between GW speed v_{GW} and EM speed v_{EM} , assuming a short difference in travel time Δt , can be characterized by:

$$\frac{\Delta v}{v_{EM}} \approx \frac{v_{EM} \Delta t}{D} \quad (3)$$

where $\Delta v = v_{GW} - v_{EM}$ and D is the distance to the source, with $D = 26 \text{ Mpc}$ (the lower bound of the 90% credibility interval for the luminosity distance of GW170817) being used. This leads to a fractional speed difference of

$$\frac{\Delta v}{v_{EM}} \in [-3 \times 10^{-15}, +7 \times 10^{-16}] . \quad (4)$$

Further observation of joint GW-GRB measurement will allow for more accurate acquisition of the speed difference, as Δt and D are the only measurements necessary for Equation 3. Current predictions state that gravitational waves propagate at exactly the speed of light, and these results lend credence to that claim [6].

Another benefit of this detection is being able to test if gravitational waves and electromagnetic radiation are affected by gravitational potentials in the same way via the Shapiro Delay:

$$\delta t_s = -\frac{1+\gamma}{c^3} \int_{\mathbf{r}_e}^{\mathbf{r}_o} U(\mathbf{r}(l)) dl \quad (5)$$

where γ is the coupling for propagation of EM or GWs to general relativity ($\gamma_{EM} = \gamma_{GW} = 1$ in Einstein-Maxwell Theory), \mathbf{r}_e and \mathbf{r}_o are the emission and observation positions, and $U(\mathbf{r})$ is the gravitational potential. By using a gravitational potential model that only considers the effect of the Milky Way outside a sphere of 100 kpc [6], a bound on $\gamma_{GW} - \gamma_{EM}$ can be found:

$$\gamma_{GW} - \gamma_{EM} \in [-2.6 \times 10^{-7}, +1.2 \times 10^{-6}] \quad (6)$$

as shown in [6]. The current best estimate of γ_{EM} is $\gamma_{EM} - 1 = (2.1 \pm 2.3) \times 10^{-5}$ found via the Shapiro delay on the Cassini spacecraft [6, 15]. Further analysis will ideally show that EM and GWs have identical couplings in general relativity.

This multi-messenger signal also allows for improvement on the value of the Hubble constant, which is well approximated for distances less than 50 Mpc:

$$v_H = H_0 D. \quad (7)$$

Using a combination of measuring the luminosity distance D via gravitational wave measurement, and acquisition of Hubble velocity v_H by electromagnetic observations; the Hubble constant can be obtained via methods that are independent of the Cosmic Microwave Background [5]. Observations from this event yield a result of $H_0 = 70.0_{-8.0}^{+12.0} \text{ km s}^{-1} \text{ Mpc}^{-1}$ [5], which is consistent from the current accepted value of $H_0 = 67.90 \pm 0.55 \text{ km s}^{-1} \text{ Mpc}^{-1}$ [7]. Additional multi-messenger binary neutron star events are expected to be detected in the coming years, allowing for higher precision in the value of H_0 .

From this merger, a value for the local coalescence rate density R of BNS systems can be obtained. This was the only merger in LIGO's second observation period with a false alarm rate below 1/100 [7]. By incorporating the local coalescence rate from the first observation period, the new rate was found to be $R = 1540_{-1220}^{+3200} \text{ Gpc}^{-3} \text{ yr}^{-1}$. This implies that the stochastic background of BNS mergers should be comparable in magnitude to the background of Binary Black Hole mergers [7].

VI. CONCLUSIONS

The BNS merger resulting in GW170817 and GRB 170817A served as a watershed moment for astronomy, as it was the first time a single source emitted both a gravitational wave and electromagnetic signal. Continued EM observation has shown support that BNS mergers are a primary source of short gamma-ray bursts. Additionally this event has allowed for a direct observation of the relative speed between gravity and light, and further BNS

mergers will allow a higher precision in that obtaining the speed of gravity. This also provides a method of acquiring the Hubble constant independent from the Cosmic Microwave Background. The results of this event show a vital importance of the global collaboration in multi-messenger astronomy, and marks a new era in gravitational wave astronomy.

- [1] Aab, A. et al. (2015). Improved limit to the diffuse flux of ultrahigh energy neutrinos from the pierre auger observatory. *Phys. Rev. D*, 91:092008.
- [2] Aartsen, M., Ackermann, M., Adams, J., Aguilar, J., Ahlers, M., Ahrens, M., Altmann, D., Andeen, K., Anderson, T., Ansseau, I., and et al. (2017a). The icecube neutrino observatory: instrumentation and online systems. *Journal of Instrumentation*, 12(03):P03012–P03012.
- [3] Aartsen, M., Ackermann, M., Adams, J., Aguilar, J., Ahlers, M., Ahrens, M., Altmann, D., Andeen, K., Anderson, T., Ansseau, I., and et al. (2017b). The icecube realtime alert system. *Astroparticle Physics*, 92:30–41.
- [4] Aasi, J. et al. (2015). Advanced LIGO. *Classical and Quantum Gravity*, 32(7):074001.
- [5] Abbott, B. P. et al. (2017a). A gravitational-wave standard siren measurement of the hubble constant. *Nature*, 551(7678):85–88.
- [6] Abbott, B. P. et al. (2017b). Gravitational waves and gamma-rays from a binary neutron star merger: GW170817 and GRB 170817a. *The Astrophysical Journal*, 848(2):L13.
- [7] Abbott, B. P. et al. (2017c). GW170817: Observation of gravitational waves from a binary neutron star inspiral. *Phys. Rev. Lett.*, 119:161101.
- [8] Abbott, B. P. et al. (2017d). Multi-messenger observations of a binary neutron star merger. *The Astrophysical Journal*, 848(2):L12.
- [9] Accadia, T. et al. (2012). Virgo: a laser interferometer to detect gravitational waves. *Journal of Instrumentation*, 7(03):P03012–P03012.
- [10] Ageron, M. et al. (2011). Antares: The first undersea neutrino telescope. *Nuclear Instruments and Methods in Physics Research Section A: Accelerators, Spectrometers, Detectors and Associated Equipment*, 656(1):11 – 38.

[11] Ahlers, M. and Halzen, F. (2018). Opening a New Window onto the Universe with IceCube. *Prog. Part. Nucl. Phys.*, 102:73–88.

[12] Albert, A. et al. (2017). Search for high-energy neutrinos from binary neutron star merger GW170817 with ANTARES, IceCube, and the pierre auger observatory. *The Astrophysical Journal*, 850(2):L35.

[13] Alexander, K. D. et al. (2017). The electromagnetic counterpart of the binary neutron star merger LIGO/virgo GW170817. VI. radio constraints on a relativistic jet and predictions for late-time emission from the kilonova ejecta. *The Astrophysical Journal*, 848(2):L21.

[14] Arcavi, I. et al. (2017). Optical emission from a kilonova following a gravitational-wave-detected neutron-star merger. *Nature*, 551:64–66.

[15] Bertotti, B., Iess, L., and Tortora, P. (2003). A test of general relativity using radio links with the cassini spacecraft. *Nature*, 425:374–376.

[16] Brown, T. M. et al. (2013). Las cumbres observatory global telescope network. *Publications of the Astronomical Society of the Pacific*, 125(931):1031–1055.

[17] Coulter, D. A. et al. (2017). Swope supernova survey 2017a (sss17a), the optical counterpart to a gravitational wave source. *Science*, 358(6370):1556–1558.

[18] Dobie, D. et al. (2018). A turnover in the radio light curve of GW170817. *The Astrophysical Journal*, 858(2):L15.

[19] Fang, K. and Metzger, B. D. (2017). High-energy neutrinos from millisecond magnetars formed from the merger of binary neutron stars. *The Astrophysical Journal*, 849(2):153.

[20] Flaugher, B. et al. (2015). The dark energy camera. *The Astronomical Journal*, 150(5):150.

[21] Goldstein, A. et al. (2017). An ordinary short gamma-ray burst with extraordinary implications: Fermi -GBM detection of GRB 170817a. *The Astrophysical Journal*, 848(2):L14.

[22] Hirata, C. (2019). Lecture 15: Gravitational waves: Astrophysical sources and detection.

[23] Kimura, S. S. et al. (2017). High-energy neutrino emission from short gamma-ray bursts: Prospects for coincident detection with gravitational waves. *The Astrophysical Journal*, 848(1):L4.

[24] Lipunov, V., Krylov, A. V., Kornilov, V. G., Borisov, G. V., Kuvshinov, D. A., Belinsky, A. A., Kuznetsov, M. V., Potanin, S. A., Antipov, G. A., Tyurina, N. V., and et al. (2004). Master: The mobile astronomical system of telescope-robots. *Astronomische Nachrichten*, 325(6-8):580–582.

[25] Lipunov, V. M. et al. (2017). MASTER optical detection of the first LIGO/virgo neutron star binary merger GW170817. *The Astrophysical Journal*, 850(1):L1.

[26] Murguia-Berthier, A. et al. (2017). A neutron star binary merger model for GW170817/GRB 170817a/SSS17a. *The Astrophysical Journal*, 848(2):L34.

[27] Savchenko, V. et al. (2017). INTEGRAL detection of the first prompt gamma-ray signal coincident with the gravitational-wave event GW170817. *The Astrophysical Journal*, 848(2):L15.

[28] Soares-Santos, M. et al. (2017). The electromagnetic counterpart of the binary neutron star merger LIGO/virgo GW170817. i. discovery of the optical counterpart using the dark energy camera. *The Astrophysical Journal*, 848(2):L16.

[29] Troja, E. et al. (2017). The X-ray counterpart to the gravitational-wave event GW170817. *Nature*, 551:71–74.

[30] Valenti, S. et al. (2017). The discovery of the electromagnetic counterpart of GW170817: Kilonova AT 2017gfo/DLT17ck. *The Astrophysical Journal*, 848(2):L24.

[31] Villar, V. A. et al. (2017). The combined ultraviolet, optical, and near-infrared light curves of the kilonova associated with the binary neutron star merger GW170817: Unified data set, analytic models, and physical implications. *The Astrophysical Journal*, 851(1):L21.